A continuation–domain decomposition algorithm for bifurcation problems *

C.-S. Chien, H.-S. Chou and B.-W. Jeng

Department of Applied Mathematics, National Chung-Hsing University, Taichung, Taiwan 402

Received 17 March 1997; revised 7 October 1999
Communicated by C. Brezinski

We study numerical solution branches of certain parameter-dependent problems defined on compact domains with various boundary conditions. The finite differences combined with the domain decomposition method are exploited to discretize the partial differential equations. We propose efficient numerical algorithms for solving the associated linear systems and for the detection of bifurcation points. Sample numerical results are reported.

Keywords: bifurcation problems, continuation methods, domain decomposition methods, finite differences

AMS subject classification: 65N06, 65F10, 65F15

1. Introduction

In this paper, we are concerned with numerical solutions of certain nonlinear eigenvalue problems of the form

$$G(u, \lambda) = 0 \quad \text{in } \Omega. \tag{1.1}$$

Here Ω is a compact domain with piecewise smooth boundary $\partial\Omega$, and one may impose appropriate boundary conditions on $\partial\Omega$. If the domain Ω possesses certain symmetries, one may solve several reduced problems of equation (1.1) on a symmetry cell Ω_1 of Ω with various boundary conditions on $\partial\Omega_1$, see, e.g., [1,14] and the further references cited therein. On the other hand, if Ω does not possess any symmetry property, then one may use the domain decomposition method to solve equation (1.1).

Suppose that equation (1.1) or its associated reduced problems are discretized by the centered difference approximations. The corresponding centered difference

* Supported by the National Science Council of R.O.C. (Taiwan) through Project NSC 89-2115-M-005-006.

analogues are of the form

$$H(x, \lambda) = 0, \tag{1.2}$$

where $H : \mathbb{R}^N \times \mathbb{R} \to \mathbb{R}^N$ is a smooth mapping with $x \in \mathbb{R}^N$, $\lambda \in \mathbb{R}$. The Jacobian of H is denoted by $DH = [D_x H, D_\lambda H] \in \mathbb{R}^{N\times(N+1)}$ with $D_x H \in \mathbb{R}^{N\times N}$. In general, the matrix $D_x H$ is symmetric if Dirichlet boundary conditions are imposed on $\partial\Omega$. On the other hand, $D_x H$ is nonsymmetric if Neumann or mixed boundary conditions are considered. The unsymmetric discretization matrices associated to a class of self-adjoint differential operators with Neumann or mixed boundary conditions are quasi-symmetric. That is, they are similar to symmetric ones. Thus, the adaptive continuation–Lanczos algorithm described in [7] can be exploited to trace solution branches of (1.2).

Our aim here is to develop efficient continuation algorithms for tracing solution curves of equation (1.2). Here the finite differences combined with the domain decomposition method [6;15, chapter 13] are exploited to discretize the partial differential equations. We show how the associated linear systems can be effectively solved, and how the bifurcation points can be detected in the context of the domain decomposition method.

This paper is organized as follows. In section 2 we show that the discretization matrices associated to a class of self-adjoint differential operators are quasi-symmetric. The implementation of the domain decomposition method in the context of continuation methods [2,3,12] is discussed in section 3. A continuation–domain decomposition algorithm is proposed for tracing solution curves of certain second order semilinear elliptic eigenvalue problems. Finally, numerical examples involving bifurcating branches of nonlinear eigenvalue problems are given in section 4.

2. Symmetrization of the discretization matrices

Exploiting symmetries in differential equations is an efficient technique to reduce the computational cost for obtaining numerical solutions of the equation. By doing this one can solve the associated reduced problems defined in a smaller domain with mixed boundary conditions, see, e.g., [1,8,14]. In general the resulting coefficient matrices are quasi-symmetric [4, p. 106]. That is, one can find some transformation matrices such that the coefficient matrices become symmetric. Thus, the continuation–Lanczos algorithm [9] can be exploited to trace solution curves of parameter-dependent problems. We refer to [10, chapter 9] and the further references cited therein for the study of the Lanczos method. Recently, a more flexible continuation–Lanczos algorithm proposed by Chien et al. is described in [7]. In this section we show that the discretization matrices associated to a class of self-adjoint differential operators are quasi-symmetric.

2.1. Discretization matrices associated to ordinary differential operators

Let T_1 and T_2 be any two unreduced real tridiagonal matrices of the following form:

$$T_i = \begin{bmatrix} a_1 & b & & & 0 \\ c_1 & a_2 & c_2 & & \\ & \ddots & \ddots & \ddots & \\ 0 & & c_{N-2} & a_{N-1} & c_{N-1} \\ & & & \alpha_i & a_N \end{bmatrix} \in \mathbb{R}^{N\times N}, \quad bc_1 > 0, \quad i = 1, 2, \quad (2.1)$$

with $\alpha_1 = c_{N-1}$, $\alpha_2 = b$ and $bc_{N-1} > 0$.

Lemma 2.1. The unreduced tridiagonal matrices T_1 and T_2 defined above are similar to the symmetric tridiagonal matrices $\widetilde{T}_1$ and $\widetilde{T}_2$ of the following form:

$$\widetilde{T}_i = \begin{bmatrix} a_1 & \sqrt{bc_1} & & & & 0 \\ \sqrt{bc_1} & a_2 & c_2 & & & \\ & c_2 & a_3 & c_3 & & \\ & & \ddots & \ddots & \ddots & \\ 0 & & & c_{N-2} & a_{N-1} & \beta_i \\ & & & & \beta_i & a_N \end{bmatrix}, \quad i = 1, 2,$$

with $\beta_1 = c_{N-1}$ and with $\beta_2 = \sqrt{bc_{N-1}}$, respectively.

Proof. Choose

$$D_1 = \operatorname{diag}\left(\sqrt{\frac{c_1}{b}}, 1, \ldots, 1\right) \quad \text{and} \quad D_2 = \operatorname{diag}\left(\sqrt{\frac{c_1}{b}}, 1, \ldots, 1, \sqrt{\frac{c_{N-1}}{b}}\right).$$

Then we have $D_1 T_1 D_1^{-1} = \widetilde{T}_1$, and $D_2 T_2 D_2^{-1} = \widetilde{T}_2$. □

Example 2.1. If we choose $a_1 = a_2 = \cdots = a_N = 2$, $b = -2$, and $c_1 = c_2 = \cdots = c_{N-1} = -1$ in (2.1), then T_1 and T_2 are the discretization matrices associated to $-\mathrm{d}^2/\mathrm{d}x^2$ defined in $[0, 1]$ with mixed boundary conditions

$$u(0) = u'(1) = 0,$$

and with Neumann boundary conditions

$$u'(0) = u'(1) = 0,$$

respectively.

Next, let P_1 and P_2 be any two real pentadiagonal matrices of the following form:

$$P_i = \begin{bmatrix} a_1 & \alpha_i & \beta_i & & & & 0 \\ b_1 & a_2 & b_2 & c_2 & & & \\ c_1 & b_2 & a_3 & b_3 & c_3 & & \\ & \ddots & \ddots & \ddots & \ddots & \ddots & \\ & & c_{N-4} & b_{N-3} & a_{N-2} & b_{N-2} & c_{N-2} \\ & & & c_{N-3} & b_{N-2} & a_{N-1} & b_{N-1} \\ 0 & & & & s & r & a_N \end{bmatrix} \in \mathbb{R}^{N\times N}, \quad i = 1, 2, \tag{2.2}$$

where $\alpha_1 = b_1,\ \beta_1 = c_1,\ \alpha_2 = p,\ \beta_2 = q$, and $b_1p,\ c_1q,\ b_{N-1}r$ and $c_{N-2}s$ are all positive numbers.

Lemma 2.2. If

$$\frac{b_1}{p} = \frac{c_1}{q} \quad \text{and} \quad \frac{b_{N-1}}{r} = \frac{c_{N-2}}{s},$$

then the matrices P_1 and P_2 defined above are similar to the pentadiagonal matrices $\widetilde{P}_1$ and $\widetilde{P}_2$ of the following form:

$$\widetilde{P}_i = \begin{bmatrix} a_1 & \gamma_i & \delta_i & & & & 0 \\ \gamma_i & a_2 & b_2 & c_2 & & & \\ \delta_i & b_2 & a_3 & b_3 & \ddots & & \\ & \ddots & \ddots & \ddots & \ddots & c_{N-3} & \\ & & c_{N-4} & b_{N-3} & a_{N-2} & b_{N-2} & \sqrt{c_{N-2}s} \\ & & & c_{N-3} & b_{N-2} & a_{N-1} & \sqrt{b_{N-1}r} \\ 0 & & & & \sqrt{c_{N-2}s} & \sqrt{b_{N-1}r} & a_N \end{bmatrix}, \quad i = 1, 2,$$

with $\gamma_1 = b_1,\ \delta_1 = c_1,\ \gamma_2 = \sqrt{b_1p},\ \delta_2 = \sqrt{c_1q}$.

Proof. Choose

$$D_3 = \operatorname{diag}\left(1, \ldots, 1, \sqrt{\frac{b_{N-1}}{r}}\right) \in \mathbb{R}^{N\times N} \quad \text{and}$$

$$D_4 = \operatorname{diag}\left(\sqrt{\frac{b_1}{p}}, 1, \ldots, 1, \sqrt{\frac{b_{N-1}}{r}}\right).$$

Then we have $D_3P_1D_3^{-1} = \widetilde{P}_1$ and $D_4P_2D_4^{-1} = \widetilde{P}_2$. □

Example 2.2. If we choose $a_1 = 5,\ a_2 = \cdots = a_{N-2} = a_N = 6,\ a_{N-1} = 7,\ b_1 = \cdots = b_{N-1} = -4,\ c_1 = \cdots = c_{N-2} = 1,\ r = -8$, and $s = 2$, then P_1 is the discretization matrix associated to $-\mathrm{d}^4/\mathrm{d}x^4$ defined on $[0, 1]$ with boundary conditions $u(0) = u''(0) = u'(1) = u'''(1) = 0$.

2.2. Discretization matrices associated to the Laplacian

Now we consider the 2-dimensional linear eigenvalue problem with Neumann boundary conditions

$$\begin{aligned} \Delta u + \lambda u &= 0 \quad \text{in } \Omega = [0,1]^2, \\ \frac{\partial u}{\partial \mathbf{n}} &= 0 \quad \text{on } \partial\Omega. \end{aligned} \tag{2.3}$$

The eigenpairs of (2.3) are

$$\begin{aligned} \lambda_{m,n} &= \left(m^2 + n^2\right)\pi^2, \\ u_{m,n}(x,y) &= \cos m\pi x \cdot \cos n\pi y, \quad m,n = 0,1,2,\ldots. \end{aligned} \tag{2.4}$$

We discretize (2.3) by the centered difference approximations with uniform mesh size $h = 1/(N-1)$ on the x- and y-axis, respectively. The discretization matrix associated to $-\Delta$ in (2.3) is denoted by $A \in \mathbb{R}^{N^2\times N^2}$, where

$$A = \frac{1}{h^2}\begin{bmatrix} A_N & -2I_N & & & 0 \\ -I_N & A_N & -I_N & & \\ & \ddots & \ddots & \ddots & \\ & & -I_N & A_N & -I_N \\ 0 & & & -2I_N & A_N \end{bmatrix} \tag{2.5}$$

with A_N obtained from h^2A by replacing A_N and I_N by 4 and 1, respectively, and $I_N \in \mathbb{R}^{N\times N}$ the identity matrix. Note that A is banded and nonsymmetric.

The eigenpairs of A are

$$\begin{aligned} \lambda^h_{m,n} &= 2(N-1)^2\left(2 - \cos\frac{m\pi}{N-1} - \cos\frac{n\pi}{N-1}\right), \\ U_{m,n}(x_i,y_j) &= \pm\cos\frac{mi\pi}{N-1}\cdot\cos\frac{nj\pi}{N-1}, \quad m,n = 0,1,\ldots,N-1, \end{aligned} \tag{2.6}$$

where $\{(x_i,y_j) \mid 0 \leqslant i,j \leqslant N-1\}$ is the set of grid points on $[0,1]^2$. Note that the eigenpairs of

$$T =: \frac{1}{h^2}\begin{bmatrix} 2 & -2 & & & 0 \\ -1 & 2 & -1 & & \\ & \ddots & \ddots & \ddots & \\ & & -1 & 2 & -1 \\ 0 & & & -2 & 2 \end{bmatrix} \in \mathbb{R}^{N\times N}$$

are (see [11, p. 440])

$$\begin{aligned} \lambda^h_n &= 2(N-1)^2\left(1 - \cos\frac{n\pi}{N-1}\right), \\ U_n &= \pm\left(\cos\frac{n\pi}{N-1}, \cos\frac{2n\pi}{N-1}, \ldots, \cos\frac{n(N-1)\pi}{N-1}\right)^{\mathrm{T}}, \quad n = 0,1,\ldots,N-1. \end{aligned} \tag{2.7}$$

Applying the idea of matrix–tensor products, one may easily verify that

$$A = I_N \otimes T + T \otimes I_N, \qquad \lambda^h_{m,n} = \lambda^h_m + \lambda^h_n, \qquad U_{m,n} = U_n \otimes U_m,$$

where $\lambda^h_{m,n}$, $U_{m,n}$ and λ^h_m, λ^h_n, U_m, U_n are defined as in (2.6) and (2.7), respectively.

Lemma 2.3. The matrix A defined in (2.5) is similar to a symmetric block tridiagonal matrix $\widetilde{A}$, where

$$\widetilde{A} = \frac{1}{h^2}\begin{bmatrix} \widetilde{A}_N & -\sqrt{2}I_N & & & & \\ -\sqrt{2}I_N & \widetilde{A}_N & -I_N & & & \\ & -I_N & \widetilde{A}_N & \ddots & & \\ & & \ddots & \ddots & -I_N & \\ & & & -I_N & \widetilde{A}_N & -\sqrt{2}I_N \\ & \mathbf{0} & & & -\sqrt{2}I_N & \widetilde{A}_N \end{bmatrix} \in \mathbb{R}^{N^2\times N^2} \tag{2.8}$$

with $\widetilde{A}_N$ obtained from $h^2\widetilde{A}$ by replacing $\widetilde{A}_N$ and I_N by 4 and 1, respectively.

Proof. Let $D = \mathrm{diag}((\sqrt{2}/2)D_5, D_5, \ldots, D_5, (\sqrt{2}/2)D_5) \in \mathbb{R}^{N^2\times N^2}$ be a block diagonal matrix, where $D_5 = \mathrm{diag}((\sqrt{2}/2), 1, \ldots, 1, (\sqrt{2}/2)) \in \mathbb{R}^{N\times N}$. One may readily verify that $DAD^{-1} = \widetilde{A}$. □

Remark. Lemmas 2.2 and 2.3 show that the symmetrizations of P_1, P_2 and A are independent of their diagonal entries.

Recently, Chien et al. [8] exploited symmetry and scaling properties of the von Kármán equations to trace solution branches of its reduced problem defined on a subdomain. Specifically, the centered difference analogue corresponding to the linearized von Kármán equations

$$\begin{aligned} \Delta^2 w + \lambda w_{xx} = 0 \quad & \text{in } \Omega_1 = \left[0, \frac{l}{2m}\right] \times \left[0, \frac{1}{2n}\right], \\ w = \Delta w = 0 \quad & \text{on } x = 0 \text{ and } y = 0, \\ w_{\mathbf{n}} = w_{\mathbf{nnn}} = 0 \quad & \text{on } x = \frac{l}{2m} \text{ and } y = \frac{1}{2n} \end{aligned} \tag{2.9}$$

is considered. Here $w(x, y)$ is the deformation of an elastic plate defined on the subdomain Ω_1 of $[0, l] \times [0, 1]$, $m, n \in \mathbb{N}$, and the subscript "**n**" denotes the unit

normal derivative. In this case the discretization matrix associated to the biharmonic operator in (2.9) is

$$B = \frac{1}{h^4}\begin{bmatrix} B_{K_1} & E_K & I_K & & & & 0 \\ E_K & B_{K_2} & E_K & I_K & & & \\ I_K & E_K & B_{K_3} & E_K & I_K & & \\ & \ddots & \ddots & \ddots & \ddots & \ddots & \\ & & I_K & E_K & B_{K_{L-2}} & E_K & I_K \\ & & & I_K & E_K & B_{K_{L-1}} & E_K \\ 0 & & & & 2I_K & 2E_K & B_{K_L} \end{bmatrix} \in \mathbb{R}^{KL\times KL} \tag{2.10}$$

with $B_{K_i} \in \mathbb{R}^{K\times K}$ obtained from h^4B by replacing E_K and I_K by -8 and 1, respectively, and

$$\begin{aligned} \operatorname{diag} B_{K_1} &= (18, 19, \ldots, 19, 20, 19), \\ \operatorname{diag} B_{K_{L-1}} &= (20, 21, \ldots, 21, 22, 21), \\ \operatorname{diag} B_{K_j} &= (19, 20, \ldots, 20, 21, 20), \quad \text{otherwise;} \end{aligned} \tag{2.11}$$

and

$$E_K = \begin{bmatrix} -8 & 2 & & & 0 \\ 2 & -8 & 2 & & \\ & \ddots & \ddots & \ddots & \\ & & 2 & -8 & \alpha \\ 0 & & & \beta & -8 \end{bmatrix} \in \mathbb{R}^{K\times K} \tag{2.12}$$

with $\alpha = 2$ and $\beta = 4$. Here the positive integers K and L in (2.10) are the number of interior mesh points on the x- and y-axis, respectively.

Lemma 2.4. The matrix B defined in (2.10) is similar to a symmetric block matrix $\widetilde{B}$. Here

$$\widetilde{B} = \frac{1}{h^4}\begin{bmatrix} \widetilde{B}_{K_1} & \widetilde{E}_K & I_K & & & & 0 \\ \widetilde{E}_K & \widetilde{B}_{K_2} & \widetilde{E}_K & I_K & & & \\ I_K & \widetilde{E}_K & \widetilde{B}_{K_3} & \widetilde{E}_K & \ddots & & \\ & \ddots & \ddots & \ddots & \ddots & I_K & \\ & & I_K & \widetilde{E}_K & \widetilde{B}_{K_{L-2}} & \widetilde{E}_K & \sqrt{2}I_K \\ & & & I_K & \widetilde{E}_K & \widetilde{B}_{K_{L-1}} & \sqrt{2}\widetilde{E}_K \\ 0 & & & & \sqrt{2}I_K & \sqrt{2}\widetilde{E}_K & \widetilde{B}_{K_L} \end{bmatrix} \in \mathbb{R}^{KL\times KL}$$

with $\widetilde{B}_{K_i} \in \mathbb{R}^{K\times K}$ obtained from $h^4\widetilde{B}$ by replacing $\widetilde{E}_K$ and I_K by -8 and 1, respectively, and the diagonal elements of $\widetilde{B}_{K_i}$ are the same as those of B_i in (2.11), and $\widetilde{E}_K$ has the same form as E_K defined in (2.12) with $\alpha = \beta = 2\sqrt{2}$.

Proof. Let $E = \text{diag}(D_6, \ldots, D_6, (\sqrt{2}/2)D_6) \in \mathbb{R}^{KL\times KL}$ be a block diagonal matrix, where $D_6 = \text{diag}(1, \ldots, 1, (\sqrt{2}/2)) \in \mathbb{R}^{K\times K}$. One may readily verify that $EBE^{-1} = \widetilde{B}$. □

Remark. One may choose D, E and D_i, $i = 1, 2, \ldots, 6$, in the proof of lemmas 2.1–2.4 so that its entries can be either positive or negative. By doing this some entries of the symmetric matrices obtained will have different signs.

3. A continuation–domain decomposition algorithm

3.1. A brief review of the predictor–corrector continuation method

We denote the discrete solutions of the equation (1.2) by c, where

$$c = \big\{y(s) = \big(x(s), \lambda(s)\big) \mid H\big(y(s)\big) = 0,\ s \in I \subset \mathbb{R}\big\}.$$

Assume that a parametrization via arc length is available on c. Several well-known curve-tracking algorithms have been developed during the past decade, e.g., the HOMPACK90 of Watson et al. [16]. We will trace the solution curve c by predictor–corrector continuation methods [2,3,12]. Numerical computation of bifurcation points and branch-switching techniques can be found, e.g., in [2,13] and the further references cited therein. Let $y_i = (x_i, \lambda_i) \in \mathbb{R}^{N+1}$ be a point which has been accepted as an approximating point for the solution curve c. Suppose that the Euler predictor is used to predict a new point $z_{i+1,1}$. That is,

$$z_{i+1,1} = y_i + \delta_i u_i. \tag{3.1}$$

Here $\delta_i > 0$ is the step length, and u_i is the unit tangent vector at y_i, which is obtained by solving the following bordered linear system:

$$\begin{bmatrix} D_x H(y_i) & D_\lambda H(y_i) \\ & r_i^{\mathrm{T}} \end{bmatrix} \cdot u_i = \begin{bmatrix} 0 \\ 1 \end{bmatrix} \tag{3.2}$$

for some constraint vector $r_i \in \mathbb{R}^{N+1}$. The accuracy of the approximation to the solution curve must be improved via a corrector process. Suppose that the modified Newton method with constraint

$$\begin{bmatrix} D_x H(z_{i+1,1}) & D_\lambda H(z_{i+1,1}) \\ & u_i^{\mathrm{T}} \end{bmatrix} \cdot w_j = \begin{bmatrix} -H(z_{i+1,j}) \\ 0 \end{bmatrix}, \quad j = 1, 2, \ldots, \tag{3.3}$$

is solved, then we set $z_{i+1,j+1} = z_{i+1,j} + w_j,\ j = 1, 2, \ldots$. If y_i lies sufficiently near c, then the modified Newton process will converge if the step size δ_i is small enough. For simplicity we rewrite the equation (3.2) or (3.3) as

$$\begin{bmatrix} A & p \\ q^{\mathrm{T}} & \gamma \end{bmatrix} \begin{bmatrix} x \\ \lambda \end{bmatrix} = \begin{bmatrix} f \\ g \end{bmatrix}, \tag{3.4}$$

where $p, q, f \in \mathbb{R}^N$ and $\gamma, g \in \mathbb{R}$. The block elimination algorithm [5,12] is given as follows.

Algorithm 3.1 (Block elimination).
Step 1. Solve $Av = p$, $Aw = f$.
Step 2. Compute $\lambda = (g - q^{\mathrm{T}}w)/(\gamma - q^{\mathrm{T}}v)$.
Step 3. Compute $x = w - \lambda v$.

3.2. The domain decomposition method

From (3.4) and algorithm 3.1 it is obvious that we need only solve one linear system to obtain the tangent vector u_i. To perform the corrector process, note that two linear systems must be solved per Newton iteration. However, one of them, namely, $D_x H(z_{i+1,1})v = D_\lambda H(z_{i+1,1})$ reappears at each iteration. Thus, after the first iteration we need only solve one linear system per iteration.

Now we discuss iterative methods for solving the linear systems in step 1 of algorithm 3.1. Without loss of generality, we consider the following semilinear elliptic eigenvalue problem:

$$\begin{aligned} \Delta u + \lambda f(u) &= 0 \quad \text{in } \Omega, \\ u &= 0 \quad \text{on } \partial\Omega. \end{aligned} \tag{3.5}$$

Here $f : \mathbb{R} \to \mathbb{R}$ is a smooth odd gradient map which is normalized to satisfy $f'(0) = 1$, $f'''(0) \neq 0$, and Ω is an L-shaped region resulting from cutting away a quarter of the unit square. Assume that edge-based partitioning is used on the domain Ω. We label the nodes by subdomain as shown in [15, p. 387]. Note that the interface nodes are labeled last. For a general partitioning into m subdomains Ω_i, $i = 1, \ldots, m$, the linear systems which appear in step 1 of algorithm 3.1 have the following form (see, e.g., [15, chapter 15]):

$$\begin{pmatrix} B_1 & & & & E_1 \\ & B_2 & & & E_2 \\ & & \ddots & & \vdots \\ & & & B_m & E_m \\ F_1 & F_2 & \ldots & F_m & C \end{pmatrix} \begin{pmatrix} r_1 \\ r_2 \\ \vdots \\ r_m \\ s \end{pmatrix} = \begin{pmatrix} d_1 \\ d_2 \\ \vdots \\ d_m \\ e \end{pmatrix}, \tag{3.6}$$

where each r_i represents the subvector of unknowns that are interior to subdomain Ω_i, and s represents the vector of all interface unknowns. We express the system (3.6) in the simpler form

$$A\begin{pmatrix} r \\ s \end{pmatrix} = \begin{pmatrix} d \\ e \end{pmatrix}, \quad A = \begin{pmatrix} B & E \\ F & C \end{pmatrix}, \tag{3.7}$$

where E represents the *subdomain* to interface coupling seen from the subdomains, F represents the interface to subdomain coupling seen from the interface nodes and $B = \text{diag}(B_1, \ldots, B_m)$ is a block diagonal matrix. Suppose that the finite difference method is used to discretize (3.5), then the matrix A is symmetric. Thus the continuation–Lanczos algorithm described in [9] can be used to solve the corresponding linear systems as well as to detect a singularity of the coefficient matrix A.

Alternatively, from the first equation of (3.7) the unknown vector r can be expressed as

$$r = B^{-1}(d - Es). \tag{3.8}$$

On substituting this into the second equation of (3.7), we obtain the following reduced system:

$$\big(C - FB^{-1}E\big)s = e - FB^{-1}d, \tag{3.9}$$

where

$$S = C - FB^{-1}E$$

is the Schur complement matrix associated with the s variable. Defining

$$E' := B^{-1}E \quad \text{and} \quad d' := B^{-1}d,$$

the solution to the linear system (3.7) is obtained by applying the block elimination once more.

Algorithm 3.2 (Block elimination algorithm for solving (3.7)).

Step 1. Solve $BE' = E$ and $Bd' = d$, respectively.

Step 2. Compute $e' = e - Fd'$.

Step 3. Compute $S = C - FE'$.

Step 4. Solve $Ss = e'$.

Step 5. Compute $r = d' - E's$.

The domain decomposition algorithm for solving (3.4) is described as follows.

Algorithm 3.3 (Domain decomposition method for solving (3.4)).

Step 1. Solve $Av = p$ and $Aw = f$ by algorithm 3.2.

Step 2. Compute $\lambda = (g - q^{\mathrm{T}}w)/(\gamma - q^{\mathrm{T}}v)$.

Step 3. Compute $x = w - \lambda v$.

In general, the matrices E_i contain a certain number of zero columns. Obviously, we can use the continuation–Lanczos algorithm in [9] to solve the symmetric linear systems with multiple right-hand sides in step 1 of algorithm 3.2 in a parallel computer. Alternatively, we can also exploit the continuation–Lanczos–Galerkin algorithm described in [7] to solve these symmetric linear systems. However, the drawback of algorithm 3.2 is that we can not detect singularities of the coefficient matrix A.

Next, we discuss direct methods for solving the linear systems in step 1 of algorithm 3.1. Recently, Allgower and Aston [1] have described numerical methods for detecting simple bifurcation points along solutions of discrete bifurcation problems, where the coefficient matrix is of the form (3.7). They proposed to use the determinant of the Jacobian as a test function since it is zero at a bifurcation point and changes sign when an odd order bifurcation point is passed. We will show that the numerical method proposed by Allgower and Aston can be used to detect multiple bifurcation points of certain semilinear elliptic eigenvalue problems as well. To start with, let

$$A = \begin{bmatrix} B & E \\ F & C \end{bmatrix}.$$

By performing an *LU*-decomposition of A, we obtain

$$\begin{bmatrix} B & E \\ F & C \end{bmatrix} = \begin{bmatrix} L_1 & 0 \\ L_2 & L_3 \end{bmatrix} \begin{bmatrix} U_1 & U_2 \\ 0 & U_3 \end{bmatrix}, \tag{3.10}$$

where L_1 and L_3 are unit lower triangular, and U_1 and U_3 are upper triangular. Expanding out the matrix product on the right-hand sides leads to the following equations:

$$B = L_1 U_1, \tag{3.11}$$

$$E = L_1 U_2, \tag{3.12}$$

$$F = L_2 U_1, \tag{3.13}$$

$$C = L_2 U_2 + L_3 U_3. \tag{3.14}$$

Equation (3.11) is simply the *LU*-decomposition for A. Once the matrices L_1 and U_1 are obtained, the matrix U_2 in (3.12) can be easily solved since L_1 is unit lower triangular. Similarly, equation (3.13) can be expressed as

$$U_1^{\mathrm{T}} L_2^{\mathrm{T}} = F^{\mathrm{T}}.$$

Therefore, L_2 can also be easily solved since U_1 is upper triangular. Finally, L_3 and U_3 can be found from an *LU*-decomposition of $C - L_2 U_2$. Now the determinant of A can be easily evaluated since $\det A = \det U_1 \cdot \det U_3$. Therefore, an odd order bifurcation point is detected on the discrete solution if the determinant of A changes sign.

For the problem (3.5), the discretization matrix A corresponding to the Laplacian is symmetric in the context of the domain decomposition method. Thus, the rank deficiency of the matrix A is revealed by the sign patterns of the diagonal entries of U_1 and U_3. Suppose that the function f in (3.5) is an odd gradient map. By the result in [2] we can detect both simple bifurcations and multiple bifurcations. This

fact has been verified by our numerical experiments. However, if the matrix A is nonsymmetric, the numerical method proposed by Allgower and Aston can no longer be exploited to detect simple bifurcations. The detailed investigation will be given elsewhere. Note that one of our main purposes is to solve the linear systems. Once we obtain the *LU*-decomposition (3.10), then (3.7) can be replaced by

$$\begin{bmatrix} L_1 & 0 \\ L_2 & L_3 \end{bmatrix} \begin{bmatrix} U_1 & U_2 \\ 0 & U_3 \end{bmatrix} \begin{bmatrix} r \\ s \end{bmatrix} = \begin{bmatrix} d \\ e \end{bmatrix}. \tag{3.15}$$

If we let

$$\begin{bmatrix} U_1 & U_2 \\ 0 & U_3 \end{bmatrix} \begin{bmatrix} r \\ s \end{bmatrix} = \begin{bmatrix} u \\ v \end{bmatrix}, \tag{3.16}$$

then from (3.15) and (3.16) we have

$$L_1 u = d, \tag{3.17}$$

$$L_2 u + L_3 v = e \quad \text{or} \quad L_3 v = e - L_2 u, \tag{3.18}$$

$$U_3 s = v, \tag{3.19}$$

$$U_1 r = u - U_2 s. \tag{3.20}$$

Combining (3.17)–(3.20), we obtain the following algorithm for solving (3.7).

Algorithm 3.4 (Detect singularity and solve the linear system (3.7)).

Step 1. Perform LU-decomposition on A, i.e.,

$$\begin{bmatrix} B & E \\ F & C \end{bmatrix} = \begin{bmatrix} L_1 & 0 \\ L_2 & L_3 \end{bmatrix} \begin{bmatrix} U_1 & U_2 \\ 0 & U_3 \end{bmatrix}.$$

Step 2. Solve $L_1 u = d$.

Step 3. Solve $L_3 v = e - L_2 u$.

Step 4. Solve $U_3 s = v$.

Step 5. Solve $U_1 r = u - U_2 s$.

Finally, algorithm 3.3 should be replaced by

Algorithm 3.5 (*LU*-decomposition for solving (3.4)).

Step 1. Solve $Av = p$ and $Aw = f$ by algorithm 3.4.

Step 2. Compute $\lambda = (g - q^{\mathrm{T}} w)/(\gamma - q^{\mathrm{T}} v)$.

Step 3. Compute $x = w - \lambda v$.

4. Numerical examples

The numerical methods described in previous sections were implemented to trace solution branches of the following second-order semilinear elliptic eigenvalue problems:

$$\begin{aligned} \Delta u + \lambda \sinh u = 0 \quad &\text{in } \Omega, \\ u = 0 \quad &\text{on } \partial\Omega. \end{aligned} \tag{4.1}$$

Equation (4.1) was discretized by the centered difference approximations with uniform mesh size $h = 0.05$ (respectively 0.025) on the x- and y-axis, respectively. In example 1, the domain decomposition method is incorporated, while in example 2, we exploit symmetry of the domain. All our computations were executed on an IBM RS/6000 SP2 machine with High Performance Fortran Compiler and with 64-bit IEEE arithmetic at National Chung Hsing University.

Example 1. We consider equation (4.1) defined on an L-shaped region described in section 3. The direct method described in section 3 is used for the associated linear systems as well as to detect a singularity of the coefficient matrix A. Figures 1–3 display the contours of the first three solution branches bifurcating at $(0, \lambda_1) \approx (0, 38.75)$, $(0, \lambda_2) \approx (0, 60.26)$, $(0, \lambda_3) \approx (0, 78.30)$, respectively.

Example 2. In this example, we show that the techniques described in section 2 can also be applied to the problem defined on a nonsquare domain. We consider equation (4.1) with $\Omega := [0, 1]^2 \setminus [0.4, 0.6]^2$. The predictor–corrector continuation method described in section 3 is exploited to trace the first few solution branches of (4.1). Our numerical results show that the solution curves of equation (4.1) bifurcating at $(0, \lambda_1)$ and $(0, \lambda_5)$ can be represented by the first two solution curves of the following reduced

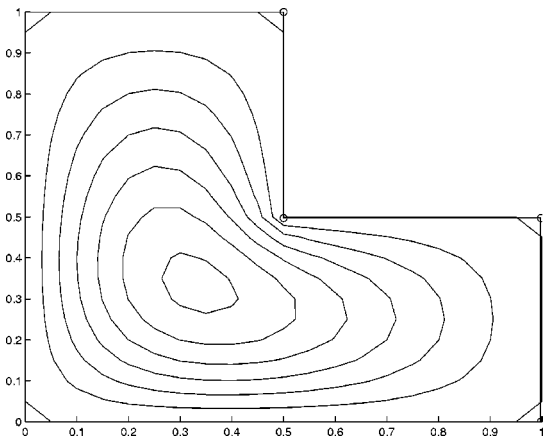

Figure 1. Contour of the solution curve bifurcating at $(0, \lambda_1) \approx (0, 38.75)$.

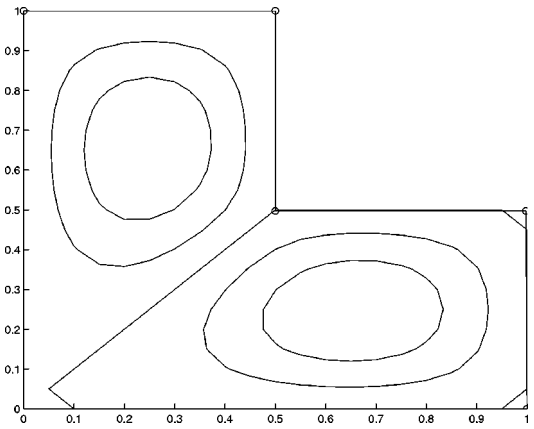

Figure 2. Contour of the solution curve bifurcating at $(0, \lambda_2) \approx (0, 60.26)$.

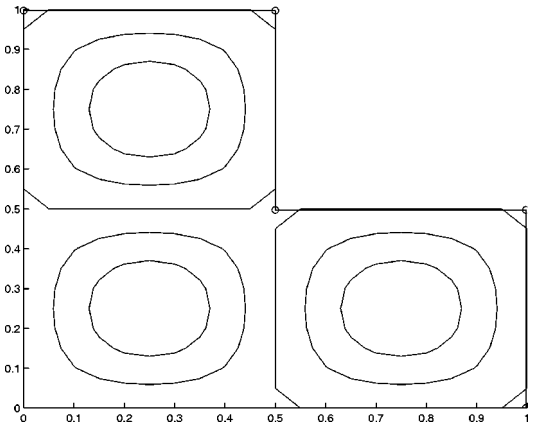

Figure 3. Contour of the solution curve bifurcating at $(0, \lambda_3) \approx (0, 78.30)$.

problem:

$$\begin{aligned} \Delta u + \mu \sinh u = 0 \quad & \text{in } \Omega' = [0, 0.5]^2 \setminus [0.45, 0.5]^2, \\ \frac{\partial u}{\partial \mathbf{n}} = 0 \quad & \text{on } x = \frac{1}{2} \text{ and } y = \frac{1}{2}, \\ u = 0 \quad & \text{on } \partial\Omega' \setminus \left\{ (x, y) \in \partial\Omega' \mid x = \frac{1}{2} \text{ or } y = \frac{1}{2} \right\} \end{aligned} \tag{4.2}$$

branching from $(0, \mu_1)$ and $(0, \mu_2)$, respectively. With $h = 0.025$ the discretization matrix associated to $-\Delta$ in (4.2) is an unsymmetric matrix of order 375×375. By using techniques similar to those described in section 2, we can show that this unsymmetric matrix is quasi-symmetric. The details are not given here. The continuation–Lanczos algorithm is exploited to trace the solution curves of (4.2). Tables 1 and 2 show that the first two bifurcation points are detected at $\mu_1 \approx 38.92546$ and $\mu_2 \approx 97.29447$,

Table 1
Sample result for example 2, $h = 0.05$, $\varepsilon = 5\cdot 10^{-8}$, $tol = 5\cdot 10^{-10}$, $\|d\|_\infty = 5\cdot 10^{-9}$, $\lambda_1 \approx 38.92683$, using the symmetric Lanczos method.

μ	MAXNORM	NCS	η	dim(T_j)	θ_1	κ_2	NCI
38.50000	0.59897E−05	7	0	11	0.15671E−02	0.49062E+04	2
38.90000	0.99027E−04	9	0	12	0.56708E−03	0.13296E+05	5
38.92449	0.11392E−02	11	0	18	0.35852E−04	0.21767E+06	6
38.92546	0.16188E−01	13	1	30	−0.10268E−05	0.76014E+07	2
38.92234	0.30977E−01	15	1	26	−0.12502E−04	0.12487E+02	2
38.84458	0.13385E+00	22	1	28	−0.32670E−03	0.19151E+02	3
37.79991	0.50053E+00	34	1	29	−0.48834E−02	0.31109E+02	5
34.51676	0.10236E+01	50	1	30	−0.21939E−01	0.35481E+03	4
29.15678	0.16177E+01	72	1	31	−0.53706E−01	0.14441E+03	4
22.55311	0.22853E+01	98	1	32	−0.10183E+00	0.75824E+02	3

Table 2
Sample result for example 2, $h = 0.05$, $\varepsilon = 5\cdot 10^{-9}$, $tol = 5\cdot 10^{-11}$, $\|d\|_\infty = 5\cdot 10^{-10}$, $\lambda_5 \approx 97.29651$, using the symmetric Lanczos method.

μ	MAXNORM	NCS	η	dim(T_j)	θ_1	κ_2	NCI
960.90000	0.81323E−06	4	0	10	0.14913E−02	0.50257E+04	3
970.25000	0.70367E−05	7	0	13	0.24128E−03	0.31140E+05	5
970.28750	0.36322E−04	9	0	15	0.53777E−04	0.13972E+06	5
970.29447	0.14970E−01	12	0	22	0.32555E−05	0.23450E+07	5
970.27858	0.44648E−01	14	2	30	−0.27837E−04	0.27512E+06	4
970.16531	0.12084E+00	18	2	27	−0.47093E−03	0.13837E+02	5
960.97100	0.19050E+00	20	2	27	−0.11021E−02	0.13892E+02	5
930.89154	0.62462E+00	36	1	24	−0.15990E−01	0.54013E+01	5
870.09788	0.11157E+01	60	1	25	−0.53021E−01	0.54665E+01	4
780.94582	0.15588E+01	88	1	26	−0.10308E+00	0.71617E+01	4

respectively. Figures 4 and 5 show the contours of these two solution curves at μ_1 and $\mu \approx 96.971$, respectively.

The following notations are used in tables 1 and 2. In order to save space, we only print out results near the bifurcation points.

NCS: numerical ordering of continuation steps,
ε: accuracy tolerance in Newton corrector,
κ_2: the two-norm condition number of coefficient matrices,
tol: stopping criterion for the CG type method,
NCI: number of corrector iterations per continuation step,
MAXNORM: maximum norm of the approximating solution,
$\|d\|_\infty$: maximum norm of the perturbation vector, see lemma 3.1.

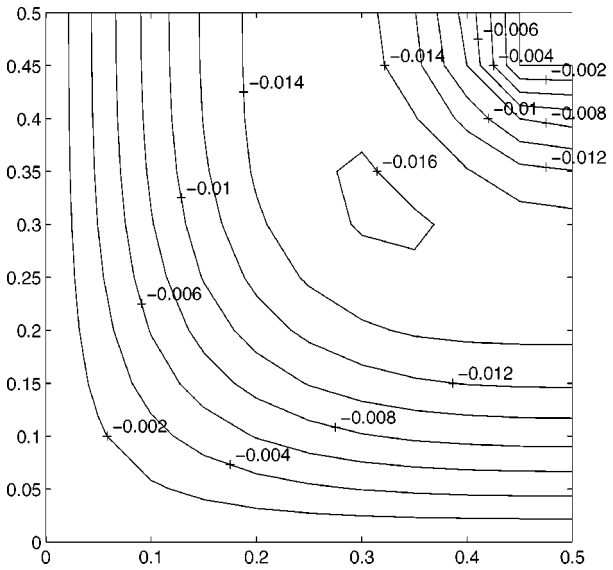

Figure 4. Contour of the solution curve at $\mu_1 \approx 38.92546$, example 2.

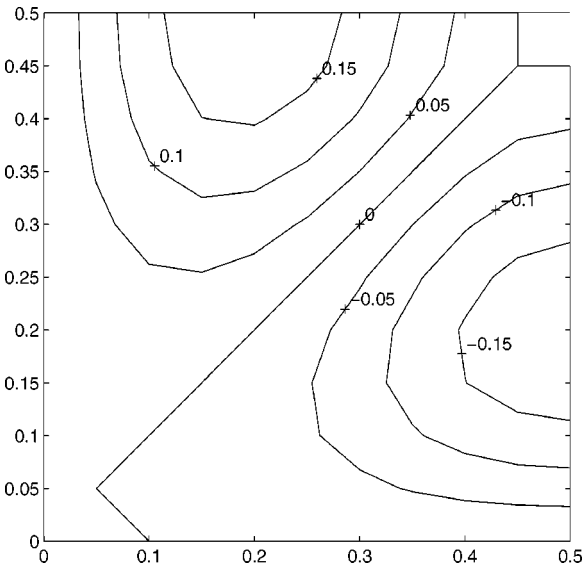

Figure 5. Contour of the solution curve at $\mu \approx 96.97100$, example 2.

Acknowledgement

We thank one anonymous referee for his criticism and suggestions that helped us improve the paper.

References

[1] E.L. Allgower and P.J. Aston, Symmetry reductions for the numerical solution of boundary value problems, in: *Lectures in Applied Mathematics* 32 (Amer. Math. Soc., Providence, RI, 1996) pp. 29–47.

[2] E.L. Allgower and C.-S. Chien, Continuation and local perturbation for multiple bifurcations, SIAM J. Sci. Statist. Comput. 7 (1986) 1265–1281.

[3] E.L. Allgower and K. Georg, Continuation and path following, Acta Numerica 2 (1993) 1–64.

[4] O. Axelsson, *Iterative Solution Methods* (Cambridge Univ. Press, Cambridge, UK, 1996).

[5] T.F. Chan, Deflation techniques and block-elimination algorithm for solving bordered singular systems, SIAM J. Sci. Statist. Comput. 5 (1984) 121–134.

[6] T.F. Chan and T.P. Mathew, Domain decomposition algorithms, Acta Numerica (1994) 61–143.

[7] C.-S. Chien, P.F. Dai and S.L. Chang, Application of the Lanczos algorithm for solving the linear systems that occur in continuation problems, to appear.

[8] C.-S. Chien, Y.-J. Kuo and Z. Mei, Symmetry and scaling properties of the von Kármán equations, J. Appl. Math. Phys. 49 (1998) 710–729.

[9] C.-S. Chien, Z.-L. Weng and C.-L. Shen, Lanczos type methods for continuation problems, J. Numer. Linear Algebra Appl. 4 (1997) 23–41.

[10] G.H. Golub and C.F. Van Loan, *Matrix Computations* (Johns Hopkins Univ. Press, Baltimore, MD, 1989).

[11] E. Isaacson and H.B. Keller, *Analysis of Numerical Methods* (Wiley, New York, 1965).

[12] H.B. Keller, *Lectures on Numerical Methods in Bifurcation Problems* (Springer, Berlin, 1987).

[13] Z. Mei, A numerical approximation for the simple bifurcation problems, Numer. Funct. Anal. Optim. 10 (1989) 383–400.

[14] Z. Mei, Path following around corank-2 bifurcation point of a semilinear elliptic problems with symmetry, Computing 47 (1991) 69–85.

[15] Y. Saad, *Iterative Methods for Large Sparse Linear Systems* (PWS Publishing Co., Boston, 1996).

[16] L.T. Watson, M. Sosonkina, R.C. Melville, A.P. Morgan and H.F. Walker, Algorithm 777: HOMPACK90: A suite of Fortran 90 codes for globally convergent homotopy algorithms, ACM Trans. Math. Software 23 (1997) 514–549.